On magnetic-field-induced non-geodesic corrections to relativistic orbital and epicyclic frequencies

Pavel Bakala, Eva Šrámková, Zdeněk Stuchlík, Gabriel Török

On magnetic-field induced non-geodesic corrections to relativistic orbital and epicyclic frequencies

Pavel Bakala, Eva Šrámková, Zdeněk Stuchlík, Gabriel Török

Institute of Physics, Faculty of Philosophy and Science, Silesian University in Opava
Bezručovo nám. 13, CZ-746 01 Opava, Czech Republic

E-mail: pavel.bakala@fpf.slu.cz

Abstract.

We discuss non-geodesic corrections to orbital and epicyclic frequencies of charged test particles orbiting a non-rotating neutron star with a dipole magnetic field. Using a fully-relativistic approach we consider influence of both the magnetic attraction and repulsion on the orbital and epicyclic motion. The magnetic repulsion introduces a rather complex and unusual behaviour of the circular orbital motion that is well defined down to the radius where the vertical epicyclic frequency looses its meaning. We demonstrate that for intensity of the magnetic interaction appropriately restricted, the stable circular orbits extend down to the magnetic innermost stable circular orbit (MISCO) that is located well under the geodetic innermost stable circular orbit (GISCO) and even can reach region under the photon circular orbit. The lowest stable circular orbit at $r_{min}^{MISCO} = 2.73M$, associated with the highest possible orbital frequency $\nu_K^{max} = 3284\,\mathrm{Hz}\,(1.5\mathrm{M}_\odot/\mathrm{M})$, corresponds to the critical value of the particle specific charge and the neutron star magnetic dipole moment product $(\tilde{\mathrm{q}}\mu)_{crit} = 1.87M^2$. For the magnetic attraction acting above the GISCO, the situation is much more simple and we demonstrate that the most significant correction arises for the radial epicyclic frequency and consequently for the location of the MISCO when strong magnetic attraction pushes its location far behind the location of GISCO. We show that the Lorentz force also naturally violates the equality of the orbital and vertical epicyclic frequencies implied by the spherical symmetry of the background Schwarzschild geometry giving rise the new effect of nodal precession of the orbital motion plane. Finally we apply the magnetic-attraction corrections on the Relativistic Precession model of the twin-peak high-frequency quasiperiodic oscillations observed in the Galactic Low Mass X-ray Binaries, showing possible high relevance of the modified radial epicyclic frequency.

PACS numbers: 95.30.Sf, 97.10.Gz, 97.10.Ld, 97.80.Jp

1. Introduction

The study of charged particles motion in strong gravitational and electromagnetic fields related to black holes and neutron stars enables us to understand the nature of the objects as well as the structure of the force fields and their role in astrophysical phenomena. The motion has been investigated both for Kerr-Newman black holes

having intrinsically coupled gravitational and electromagnetic fields and for strong gravitating objects (black holes and neutron stars) with a test electromagnetic field influenced by gravity (see, e.g., Johnston & Ruffini, 1974; Prasanna & Vishveshwara, 1978; Prasanna, 1980; Calvani et al., 1982; Balek et al., 1989; Bičák et al., 1989; Vokrouhlický & Karas, 1991; Stuchlík & Hledík, 1998; Stuchlík et al., 1999; Abdujabbarov & Ahmedov, 2009).

It has been shown that magnetic fields around a rotating black hole could be related to the extraction of the rotation energy from the black hole through the so-called Blandford-Znajek process enabling formation of the relativistic jets along the black hole rotation axis (Blandford Znajek, 1977). Motion of charged particles in the magnetic field generated by accretion discs orbiting black holes was discussed in (Znajek, 1976; Mobarry & Lovelace, 1986). On the other hand, the magnetic field tied to a neutron star could substantially influence the structure of an equatorial accretion disc orbiting the neutron star. Here we focus attention on the equatorial orbital and epicyclic motion in the combined gravitational and dipole magnetic fields related to a slowly rotating neutron star. Its spacetime is represented by the Schwarzschild geometry that influences the structure of the dipole magnetic field.

In the case of motion in test fields on strong gravity backgrounds, the equations of motion are complex and have to be integrated numerically (Prasanna & Vishveshwara, 1978; Prasanna & Sengupta, 1994; Preti, 2004). Quite recently, off-equatorial circular orbits were discussed in astrophysically relevant situations (Kovář et al., 2008; Stuchlík et al., 2009b). Of high interest is the equatorial motion, especially the circular and quasi-circular orbits that seem to be crucial from the point of view of accretion processes. Numerical integration of the motion equations gives a number of interesting results, but is not sufficient for a complete classification and understanding of the motion in the equatorial plane. In order to extend the understanding of the charged particle motion, we consider for the first time its very important aspect, namely the quasi-circular equatorial epicyclic motion corresponding to oscillations of particles around stable circular orbits. It is quite interesting that such epicyclic motion can be excited in the innermost parts of the accretion discs orbiting a neutron star by inhomogeneities (mountains) on its surface (Stuchlík et al., 2008).

The epicyclic motion could be relevant in modelling the high-frequency quasi-periodic oscillations (QPOs) that have been detected during the past two decades from a number of Low-Mass X-Ray Binaries (LMXBs)‡ containing a neutron star. These oscillations occur at frequencies lying in the kHz range and often come in pairs of the lower and upper QPO mode with frequencies ν_L, ν_U, forming the so-called twin-peak QPOs. Notably, ν_L, ν_U roughly correspond to Keplerian periods in the close vicinity of the binary compact object; see, e.g., van der Klis (2006). Moreover, there are indications that the twin-peak frequencies are clustered near rational ratios that are mostly around 3:2, but also 4:3 and 5:4 ratios (see, e.g., Török et al., 2008a,b,c)).

‡ binary systems containing a neutron star where the companion mass is smaller than the mass of the neutron star

Miscellaneous orbital QPO models have been proposed (see, e.g., Lamb et al., 2007; Aschenbach , 2007; Miller, 2007). In particular, the relativistic precession (RP) model (Stella & Vietri, 1999) relates the upper and lower kHz QPOs to the Keplerian and periastron precession frequency on a geodesic orbit located in the inner part of the accretion disc §. It has been noticed that, in general, correlation $\nu_U(\nu_L)$ is qualitatively well-fitted by the RP model prediction (see, e.g., Stella & Vietri, 1999, 2002; Belloni et al., 2007). There are, however, another QPO models based on the oscillations of toroidal discs (Šrámková et al., 2005; Straub & Šrámková, 2009) or "discoseismology" (Kato et al., 1998; Pétri, 2005) and so far no definite agreement on the validity of the QPO models has been established. Let us stress that the orbital and epicyclic frequencies, that will be discussed in the present paper, play an important role in all of the mentioned QPO models.

When modelling individual frequency relations from the RP model, mass and angular momentum relevant to the best fits are questionably high ($M \sim 2 \div 3M_\odot,\ j \sim 0.2 \div 0.4$); (see, e.g., Stella & Vietri, 2002; Boutloukos et al., 2006; Belloni et al., 2007; Török et al., 2007a) in comparison with the "canonical value", $M \sim 1.4M_\odot$, which has been estimated for a variety of well-studied pulsars (e.g., Glendenning, 1997; Weber, 1999). Also, quality of the fits is not satisfactory with chi-square indicating a systematic deviation between the expected and empirical trend (Belloni et al., 2007; Török et al., 2007a,b). In fact, we show that both discrepancies can be corrected by non-geodesic corrections of the orbital and epicyclic frequencies using the magnetic attraction introduced in the present paper. On the other hand, the magnetic repulsion makes the situation worse due to the shift to higher frequencies (neutron star masses).

In the present paper we discuss in detail the non-geodesic, magnetic corrections to the epicyclic motion using a fully general relativistic approach. These corrections are assumed to be implied by the Lorentz force acting on a slightly charged matter in the approximation of a spherically symmetric spacetime. We focus consideration to the case of motion in the field of magnetized neutron stars. We use the approximation of a dipole magnetic field whose axis of symmetry coincides with the axis of neutron star's rotation. The spacetime outside the neutron star is described by the Schwarzschild geometry and the effects of frame-dragging and contribution of the electromagnetic field to the stress-energy tensor are thus neglected ‖. Such approximation is suitable for describing the charged particles motion around slowly rotating neutron stars with a relatively weak magnetic field which does not affect the spacetime curvature in the vicinity of the neutron star, but its structure is governed by the neutron star spacetime structure ¶.

§ A similar model relates the low-frequency QPO branch to the "Lense–Thirring" orbit precession; see, e.g., Stella & Vietri (1998).

‖ More general and accurate approximation which takes into account the effects of frame-dragging and declination of the dipole magnetic field symmetry axis can be found in (Rezzolla et al., 2001a,b).

¶ The neutron star magnetic field is however fully dominant over the magnetic field generated by the currents in the disc.

Epicyclic motion and the related frequencies have so far been extensively discussed for the quasi-circular geodesic motion (see, e.g., Aliev & Galtsov, 1981; Abramowicz & Kluźniak, 2005; Török & Stuchlík, 2005). Using the approach of Aliev (2008), we turn attention for the first time to a detailed study of magnetically influenced perturbative epicyclic motion around equatorial circular orbits. We calculate the relevant frequencies of the non-geodesic charged test particles motion and the corresponding shift of the position of the innermost stable circular orbit that is governed by vanishing of the radial (vertical) epicyclic frequency. We consider both the cases of magnetic attraction when the innermost stable orbit is shifted above the GISCO and magnetic repulsion when it is shifted below the geodesic orbit. We find a variety of interesting new phenomena of the epicyclic motion, with unusual behaviour of the epicyclic frequencies and their relation to the orbital (Keplerian) frequency. We also discuss some implications of the magnetic attraction case for the RP model, in particular the remarkable lowering of the neutron star mass estimation obtained by fitting the QPO observational data.

2. Circular orbital motion in a dipole magnetic field on the Schwarzschild background

The line element in the Schwarzschild spacetime has the familiar form

$$\mathrm{d}s^2 = -\eta(r)^2\mathrm{d}t^2 + \frac{\mathrm{d}r^2}{\eta(r)^2} + r^2(\mathrm{d}\theta^2 + \sin^2\theta\,\mathrm{d}\phi^2)\,, \tag{1}$$

where $\eta(r)$ is given by

$$\eta(r) \equiv \left(1 - \frac{2M}{r}\right)^{1/2}. \tag{2}$$

We have adopted here geometric units, $c = G = 1$, that we will use throughout the paper, if not stated otherwise.

Solving the vacuum Maxwell equations

$$F^{\mu\nu}_{\ ;\mu} = 0 \qquad ({}^*F^{\mu\nu}_{\ ;\mu} = 0) \tag{3}$$

on the background of the spacetime geometry (1) for a static magnetic dipole moment μ, parallel to the rotational axis of the star, one obtains the formula for an exterior ($r > R$, where R is the neutron star radius) four-potential A_μ (e.g., Wasserman & Shapiro , 1983; Braje & Romani, 2001),

$$A_\alpha = -\,\delta^\phi_\alpha\, f(r)\frac{\mu\sin^2\theta}{r}\,, \tag{4}$$

which has the form of the flat space result, multiplied by a function $f(r)$ given by

$$f(r) = \frac{3r^3}{8M^3}\left[\log\eta(r)^2 + \frac{2M}{r}\left(1 + \frac{M}{r}\right)\right]. \tag{5}$$

In the case of potential (4), the Maxwell tensor $F_{\mu\nu}$, connected to the four-potential A_μ through the relation

$$F_{\mu\nu} = \frac{\partial A_\nu}{\partial x^\mu} - \frac{\partial A_\mu}{\partial x^\nu}, \tag{6}$$

has only two independent non-vanishing components,

$$F_{r\phi} = \frac{\mu \sin^2\theta \, (f(r) - r f'(r))}{r^2} \tag{7}$$

and

$$F_{\theta\phi} = -\frac{\mu f(r) \sin 2\theta}{r}, \tag{8}$$

which are related to components of a magnetic field three-vector B as follows:

$$F_{r\phi} = B^\theta \, , \, F_{\theta\phi} = -B^r \, . \tag{9}$$

Note that "coma" in Eq. (7) denotes partial derivative with respect to the radial coordinate r.

In a curved spacetime with presence of an electromagnetic field, the equation of motion for a charged test particle of mass m and charge q reads

$$\frac{\mathrm{d}U^\mu}{\mathrm{d}\tau} + \Gamma^\mu_{\alpha\beta} U^\alpha U^\beta = \tilde{\mathrm{q}} \, F^\mu_\nu U^\nu \tag{10}$$

where U^μ is the four-velocity and $\tilde{\mathrm{q}} \equiv q/m$ is the specific charge of the particle.

We shall study epicyclic, near circular motion in the equatorial plane of a neutron star with a dipole magnetic field. In order to obtain maximal information on the epicyclic motion, we shall consider its properties down to minimal radius $R = 2.25M$ allowed for internal Schwarzschild geometry with uniform energy density distribution (Stuchlík, 2000). On the other hand, we put limit of validity of our result in the field of astrophysically plausible neutron stars using the minimal radius $R \sim 3.5M$ allowed for a variety of realistic equations of state (see Appendix for details). The Lorentz force in the equation of motion, and consequently the described effects on the orbital motion, depend on the product of μ and $\tilde{\mathrm{q}}$ determining magnitude of the magnetic interaction. Therefore, instead of changing magnitude and orientation of μ we can, without any loss of generality, study only influence of changes of the specific charge $\tilde{\mathrm{q}}$. We shall focus on a typical LMXBs neutron star with a relatively weak magnetic field strength $B = 10^7$ *Gauss*, mass $M = 1.5 M_\odot$ and radius $R = 4M$. Then the magnetic dipole moment $\mu = 1.06 \, \mathrm{x} \, 10^{-4} \, m^2$ and it changes linearly with the field strength B (see Appendix). In order to keep the magnetic force fixed, the specific charge $\tilde{\mathrm{q}}$ must be changed inversely to changes of B, if the neutron star parameters R and M remain fixed.

2.1. Orbital angular velocity of equatorial circular orbits

Symmetry properties of the spacetime geometry (1) and electromagnetic field (4) allow for charged test particles motion restricted to the equatorial plane $\theta = \pi/2$. Throughout this paper we confine ourselves to studying only circular equatorial motion [+]. The four-velocity then has only two non-vanishing components, $U^\mu = (U^t, 0\,, 0\,, U^\phi)$. Solving the radial component of Eq. (10) together with the normalization condition $U^\mu U_\mu = -1$ for

[+] See Kovář et al. (2008) for discussion of the existence of non-equatorial, so called "halo", orbits.

metric (1) and potential (4) we obtain two pairs of the nonzero components of U^μ in the form

$$U^\phi_\pm = \frac{-\tilde{\mathrm{q}}\,\mu\,\chi\,(r)\;\pm\;\Psi\,(r)}{2r^3\,(r-3M)}\,, \tag{11}$$

$$U^t_\pm = \sqrt{\frac{r-\tilde{\mathrm{q}}\,\mu\,\Phi(r)\,U^\phi_\pm}{(r-3M)}}\,, \tag{12}$$

and the appropriate angular velocities $\Omega_\pm = U^\phi_\pm/U^t_\pm$ then read

$$\Omega_\pm = \frac{-\tilde{\mathrm{q}}\,\mu\,\chi\,(r) \pm \Psi\,(\mathrm{r})}{r^{3/2}\sqrt{4r^4\,(r-3M)\;-\;2\tilde{\mathrm{q}}\,\mu\Phi\,(r)\,[-\tilde{\mathrm{q}}\,\mu\,\chi\,(r)\pm\Psi\,(\mathrm{r})]}} \tag{13}$$

Here $\Phi(r)$, $\chi(r)$ and $\Psi(r)$ are given by

$$\Phi(r) \equiv f(r) - rf'(r)\,, \tag{14}$$

$$\chi(r) \equiv (r-2M)\;\Phi(r)\,, \tag{15}$$

$$\Psi(r) \equiv \sqrt{4Mr^4(r-3M) + \left(\tilde{\mathrm{q}}\mu\,\chi(r)\right)^2}\,. \tag{16}$$

For uncharged particles we arrive at the Keplerian geodesic limit with orbital angular velocity $\Omega_\pm(\tilde{\mathrm{q}}=0) = \pm\Omega_K = \pm\sqrt{M/r^3}$.

The constants of motion of charged particles at the equatorial circular orbits are given by the relations

$$E = -U_t = \eta(r)^2\,U^t, \tag{17}$$

$$L = U_\phi + \tilde{\mathrm{q}}\,A_\phi = r^2\,U^\phi - \tilde{\mathrm{q}}\,\mu\,\frac{f(r)}{r} \tag{18}$$

with E being the specific energy and L being the generalized specific angular momentum.

It is apparent from the form of Eqs (11 - 13) that for a fixed magnetic dipole moment of the neutron star, the 4-velocity components $U^\phi_\pm$ and $U^t_\pm$ are symmetric with respect to simultaneous interchange of their sign (orientation of the orbital angular velocity Ω) and the sign of the specific charge $\tilde{\mathrm{q}}$. It is therefore sufficient to analyse only one of these solutions - in the following we choose U^ϕ_+, U^t_+ and Ω_+.

The existence of the circular orbits is limited by the condition that both U^t_+ and U^ϕ_+, defined by Eqs(11) and (12), take real values. The reality conditions related to the magnitude of the magnetic interaction given by $\tilde{\mathrm{q}}\,\mu$ are given by the relations

$$4r^4\,(r-3M)\;-\;2\tilde{\mathrm{q}}\,\mu\Phi\,(r)\,[-\tilde{\mathrm{q}}\,\mu\,\chi\,(r)\pm\Psi\,(\mathrm{r})] > 0 \tag{19}$$

and

$$4Mr^4(r-3M) + \left(\tilde{\mathrm{q}}\mu\,\chi(r)\right)^2 > 0\,. \tag{20}$$

The first of these conditions is satisfied for all values of $\tilde{\mathrm{q}}\,\mu$ at all radii $r > 2M$. The second condition puts limit on the allowed values of $\tilde{\mathrm{q}}\,\mu$ at radii $2M < r < 3M$. The limit region starts for $\tilde{\mathrm{q}}\,\mu = 0$ at $r = 3M$, reaches its maximum of $\tilde{\mathrm{q}}\,\mu = \pm\,1.971\,M^2$ at $r = 2.441M$ and takes the value of $\tilde{\mathrm{q}}\,\mu = \pm\,1.333\,M^2$ for $r \to 2M$.

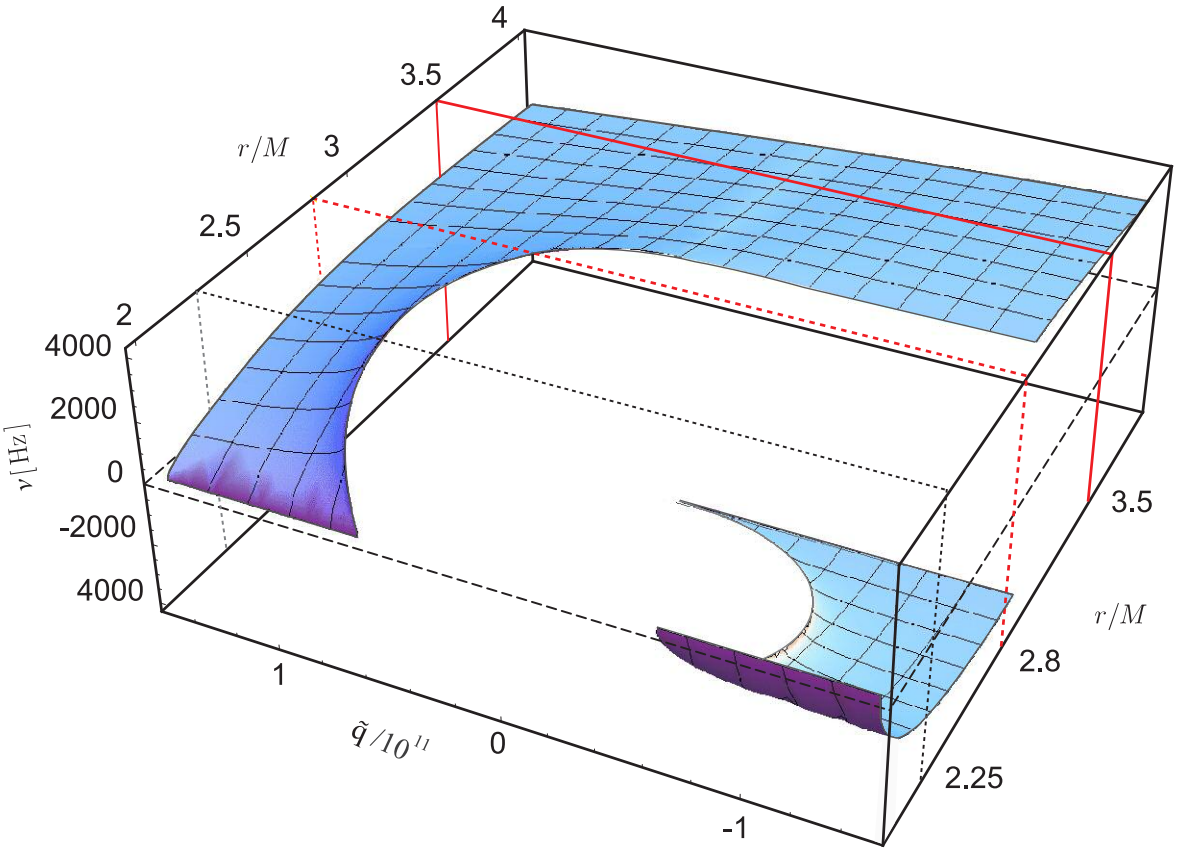

Figure 1. The orbital frequency $\nu = \Omega/2\pi$ as a function of the specific charge $\tilde{\mathrm{q}}$ and radial coordinate for the test neutron star with $M = 1.5M_\odot$ and $\mu = 1.06\,\mathrm{x}\,10^{-4}\,m^2$.

In Fig.1 we illustrate behaviour of the orbital angular velocity Ω (related frequency $\nu = \Omega/2\pi$) in dependency on the specific charge $\tilde{\mathrm{q}}$ for fixed magnetic dipole moment $\mu = 1.06\,\mathrm{x}\,10^{-4}\,m^2$ and neutron star mass $M = 1.5M_\odot$. For such a value of μ, the critical values of the specific charge are given by $\tilde{q} = \pm 8.986\,\mathrm{x}\,10^{10}$ at $r = 2.441M$ and by $\tilde{q} = \pm 6.8\,\mathrm{x}\,10^{10}$ for $r \to 2M$. From Fig.1 it follows that for positively charged particles the Lorentz force has a repulsive character and lowers the orbital frequency Ω with respect to the Keplerian frequency Ω_K corresponding to the geodesic motion ($\tilde{\mathrm{q}} = 0$), while for negatively charged particles the force is attractive and Ω grows with respect to Keplerian frequency Ω_K.

Considering both attractive and repulsive character of the Lorentz force, there exist three qualitatively different types of the orbital angular velocity Ω profile behaviour. For a sufficiently small charge, corresponding to orbital motion that is not very far from the geodesic motion, there is a minimum possible value of r for which the circular orbits may exist. With increasing magnitude of the specific charge (both positive and negative), there appears a second region of the existence of circular orbits close to the horizon with a certain maximal value of the radial coordinate. With growing charge both regions merge and circular orbits exist for all $r > R_g$. A surprising behaviour of Ω arises for negatively charged particles under the circular photon orbit at $r_{ph} = 3M$ since they orbit

in the opposite direction as compared to those orbiting above r_{ph}. (A similar effect was investigated by Balek et al. (1989) for ultrarelativistic charged particles orbiting in the field of Kerr-Newman black holes.) We should stress, however, that for astrophysically plausible situations, with neutron stars modelled by using realistic equations of state, validity of our results, being restricted to exterior regions of the neutron stars, is limited to $r > 3.5M$, or $r > 2.8M$ in the most exotic case of the so called Q-stars (see Appendix).

The test particle motion in combined gravitational and magnetic fields can be described by the effective potential $V_{eff}(r, \theta)$ generally determining 3D motion that is reduced to 2D motion in the symmetry (equatorial) plane. Examples of such effective potential corresponding to our discussion can be found in Aliev & Galtsov (1981); Kovář et al. (2008). The epicyclic motion along a stable circular orbit, given by the condition $dV_{eff}/dr = 0$, is governed by the second derivatives of the effective potential. In such approximation the effective potential takes the form corresponding to the linear harmonic oscillation, therefore, the radial and vertical epicyclic frequencies are related to the effective potential by

$$\omega_r^2 \sim \frac{\partial^2 V_{eff}}{\partial r^2}\,, \qquad \omega_\theta^2 \sim \frac{\partial^2 V_{eff}}{\partial \theta^2}\,. \tag{21}$$

Clearly, vanishing of the radial ω_r and vertical ω_θ epicyclic frequencies generally determines the marginally stable circular orbits that are defined by vanishing of the second derivatives of the effective potential, putting thus limits on the existence of astrophysically important stable circular orbits.

A detailed analysis of the effective potential that can give an overview of the stability for the charged particle circular motion can be found, e.g., in Kovář et al. (2008), even for off-equatorial circular orbits. Here we use a more straightforward and simple perturbative analysis of the epicyclic motion along equatorial stable circular orbits.

3. Epicyclic frequencies and stability of circular motion

Formulae for the radial and vertical epicyclic frequencies of a charged test particle in the presence of a general electromagnetic field have been derived by Aliev & Galtsov (1981); Aliev (2008). One may obtain the formulae by perturbing the particle's position around the equatorial circular orbit $(r, \theta) = (r_0, \pi/2)$, i.e., by assuming that $x^\mu(\tau) = z^\mu(\tau) + \xi^\mu(\tau)$ where $\xi^\mu(\tau)$ is a small perturbation. Substituting this into the equation of motion (10) and restricting to first-order terms in ξ^μ one arrives at the relation for ξ^μ that takes the form of equation for a linear harmonic oscillator

$$\frac{d^2\xi^a}{dt^2} + \omega_a^2 \xi^a = 0, \quad a \in (r, \theta) \tag{22}$$

with the appropriate epicyclic angular frequencies defined as (Aliev, 2008)

$$\omega_r = \left(\frac{\partial V^r}{\partial r} - \gamma^r_A \gamma^A_r\right)^{1/2}, \quad A \in (t, \phi) \tag{23}$$

$$\omega_\theta = \left(\frac{\partial V^\theta}{\partial \theta}\right)^{1/2}, \tag{24}$$

where γ^{μ}_{α} and V^{μ} have the form

$$\gamma^{\mu}_{\alpha} = 2\Gamma^{\mu}_{\alpha\beta}U^{\beta}(U^t)^{-1} - \frac{\tilde{\mathrm{q}}}{U^t}\,F^{\mu}_{\alpha}\,, \tag{25}$$

$$V^{\mu} = \frac{1}{2}\left[\gamma^{\mu}_{\alpha}U^{\alpha}(U^t)^{-1} - \frac{\tilde{\mathrm{q}}}{U^t}\,F^{\mu}_{\alpha}U^{\alpha}(U^t)^{-1}\right]. \tag{26}$$

Note that the derivatives in Eqs.(23) and (24) must be taken at the appropriate equatorial circular orbit $(r,\theta) = (r_0, \pi/2)$ with U^t and U^{ϕ} given by Eqs. (12) and (11).

In the spacetime geometry (1) and the magnetic field (4), the explicit expressions for the epicyclic angular frequencies are given by

$$\begin{aligned}\omega_r^2 = &\Big\{\left(U^{\phi}\right)^2 r^6(3r-8M) + 2M(M-r)r^3\left(U^t\right)^2 \\ &+ \tilde{\mathrm{q}}\,\mu\,\Big[\Phi(r)\left(2U^{\phi}r^3(3r-7M) + \tilde{\mathrm{q}}\,\mu\,\chi(r)\right) \\ &+\; U^{\phi}r^5(r-2M)f''(r)\Big]\Big\}\Big/ r^7\left(U^t\right)^2\,,\end{aligned} \tag{27}$$

$$\omega_{\theta}^2 = \frac{U^{\phi}\left(U^{\phi}r^3 - 2\tilde{\mathrm{q}}\,\mu\,f\,(r)\right)}{\left(U^t\right)^2 r^3}. \tag{28}$$

One can easily check that in the absence of the Lorentz force ($\mu = 0$ or $\tilde{\mathrm{q}} = 0$) the expressions for the orbital (13) and epicyclic (27, 28) frequencies merge into the well-known formulae for geodesic motion in the Schwarzschild geometry:

$$\Omega = \omega_{\theta} = \Omega_K = \sqrt{M/r^3}\,, \quad \omega_r = \sqrt{M(r-6M)}/r^2. \tag{29}$$

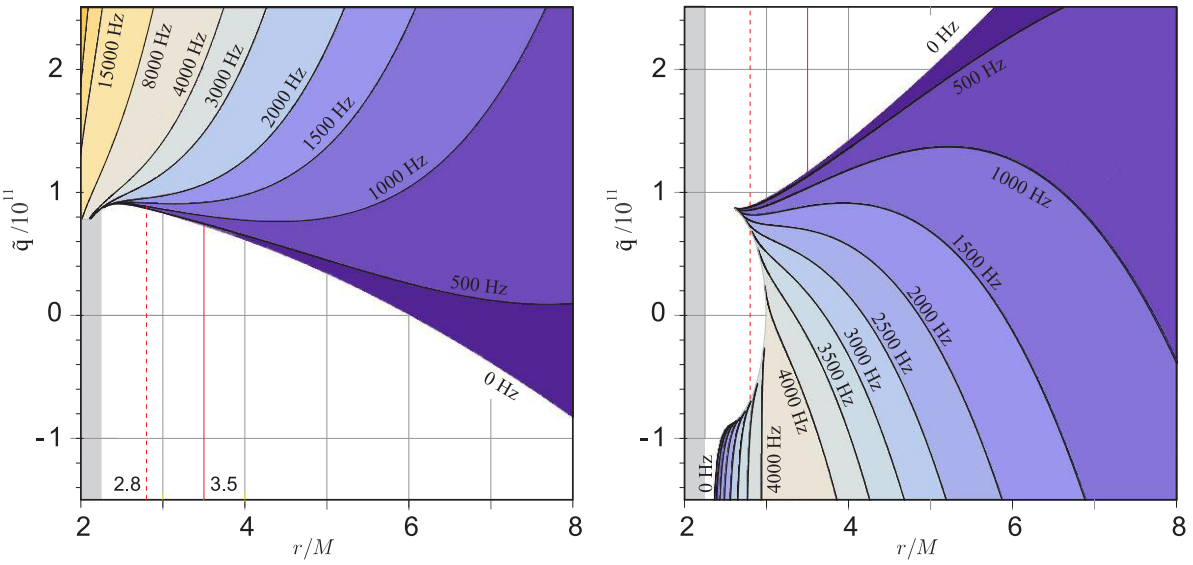

Figure 2. Left: Contour plot of the radial epicyclic frequency $\nu_{\mathrm{r}} = \omega_r/2\pi$ as a function of the specific charge $\tilde{\mathrm{q}}$ and the radial coordinate. Right: Same as the left panel, but for the vertical epicyclic frequency $\nu_{\theta} = \omega_{\theta}/2\pi$. Plots are constructed for the test neutron star with $M = 1.5M_{\odot}$ and $\mu = 1.06\,\mathrm{x}\,10^{-4}\,m^2$.

3.1. Radial epicyclic frequency

In the context of the perturbation analysis, the existence of real values of the radial epicyclic frequency ω_r implies the stability of the circular orbit with respect to small radial perturbations (which lead to oscillation behaviour of the perturbed radial coordinate of the orbiting particle). In the left panel of Fig. 2, the line of $\omega_r = 0$ in the $\tilde{\mathrm{q}} - r$ plane denotes the boundary of region where the stable circular orbits exist. Outside this region the appropriate ($a = r$) solution of Eq. (22) looses its oscillatory character. In the region corresponding to attractive Lorentz force ω_r decreases with growing $\tilde{\mathrm{q}}$ and the marginally stable orbit with respect to radial oscillations moves away from the analogous orbit in the purely geodesic case, $r_{ms} = 6M$. On the other hand, in the region of the repulsive Lorentz force ω_r grows as the negative charge $\tilde{\mathrm{q}}$ increases and the boundary of region with "radially stable" orbits approaches the horizon where ω_r diverges to infinity.

3.2. Vertical epicyclic frequency

Analogically, the existence of the vertical epicyclic frequency implies the stability of the circular orbit with respect to small vertical perturbations. The region where such stable circular orbits may exist is shown in the right panel of Fig. 2. As seen from the Figure, the behaviour of ω_θ exhibits a bit more complicated features than it was in the case of ω_r. There are two separate curves of $\omega_\theta = 0$ defining a part of the boundary of region with circular orbits that are stable with respect to vertical perturbations. One of the curves lies in the area of repulsive Lorentz force, while the other one corresponds to area with attractive character of the Lorentz force. Contrary to the radial case, this region of "vertical stability" never reaches the horizon. For relatively small values of both positive and negative charge corresponding to near geodesic motion, the rest of the boundary of the region where the vertically stable circular orbits exist coincides with the boundary of region defining the existence of circular orbits itself (see Fig. 1).

3.3. Stable orbits and magnetic innermost stable circular orbit (MISCO)

Clearly, stable orbits have to be stable to both radial and vertical perturbations simultaneously. From the above discussion of behaviour of the radial and vertical epicyclic frequency it is apparent that the region of circular orbits which are stable with respect to both radial and vertical perturbations is defined by the intersection of regions where the radial and vertical epicyclic frequencies are defined. As shown in the left panel of Fig.3, there exists a critical value of the specific charge, $\tilde{\mathrm{q}}_{crit}$, inside the area of the repulsive Lorentz force, such that for $\tilde{\mathrm{q}} > \tilde{\mathrm{q}}_{crit}$ the boundary of the region of stable orbits in the $\tilde{\mathrm{q}}$ - r plane is defined by the $\omega_\theta = 0$ curve. For $\tilde{\mathrm{q}} < \tilde{\mathrm{q}}_{crit}$, the boundary of stable orbits region is formed by the curve of $\omega_r = 0$. These curves thus define the location of the marginally stable orbit for particles of a given $\tilde{\mathrm{q}}$ with a fixed μ. For such orbits we introduce the term MISCO (Magnetic Innermost Stable Circular

Orbit) to distinguish them from the corresponding geodesic innermost stable circular orbits that we will refer to as GISCO. In the Schwarzschild spacetimes $r_{GISCO} = 6M$. It is, therefore, clear that the repulsive Lorentz force gives rise to a new class of stable circular orbits with $r < r_{GISCO} = 6M$ that extends below the circular photon orbit. The critical charge $\tilde{\mathrm{q}}_{crit}$ corresponds to the lowest MISCO orbit with radial coordinate $r^{\mathrm{MISCO}}_{min} = 2.73M$ and the highest possible orbital angular frequency Ω^{max} for a given mass of the neutron star. The location of MISCO_{min} orbit is given by the condition that equations $\omega_r = 0$ and $\omega_\theta = 0$ are fulfiled simultaneously, the critical value of the product of the particle specific charge and the neutron star magnetic dipole moment is thus given by $(\tilde{\mathrm{q}}\mu)_{crit} = 1.869M^2$. For the test neutron star of $M = 1.5M_\odot$ and $\mu = 1.06\,\mathrm{x}\,10^{-4}\,m^2$, we have $\tilde{\mathrm{q}}_{crit} = 8.76\,\mathrm{x}\,10^{10}$ and $\nu^{max} = \Omega^{max}/2\pi = 3124$ Hz.

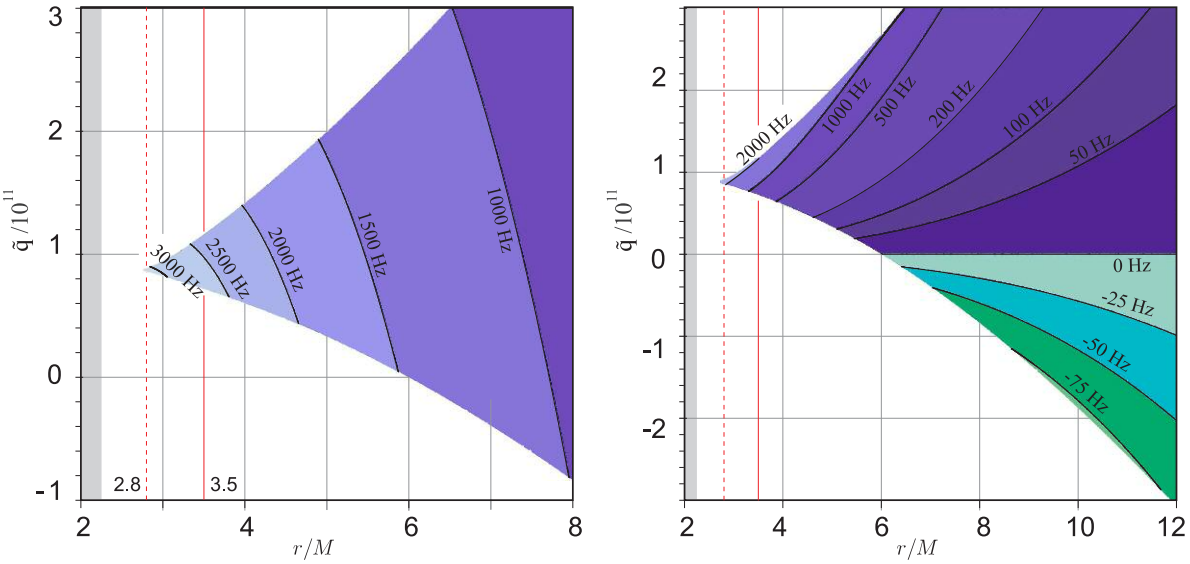

Figure 3. Left: The region of stable circular orbits filled up by the contour plot of the orbital frequency $\nu = \Omega/2\pi$. Right: Same as the left panel, but filled up by the contour plot of the nodal precession frequency ν_{n}. Constructed for $M = 1.5M_\odot$ and $\mu = 1.06\,\mathrm{x}\,10^{-4}\,m^2$.

4. Relations of the non-geodesic orbital and epicyclic frequencies

The orbital and epicyclic frequencies exhibit a qualitatively different behaviour in regions of attractive and repulsive magnetic interaction that strongly depends on the particular value of $\tilde{q}$. For the test neutron star we present in Fig.4 non-geodesic orbital and epicyclic frequency profiles in typical situations representing both the repulsive attractive magnetic interaction. In the region of magnetic repulsion ($\tilde{\mathrm{q}} > 0$) two qualitatively different types of the frequency profile behaviour are given by conditions $\tilde{\mathrm{q}} > \tilde{\mathrm{q}}_{\mathrm{crit}}$ ($\tilde{\mathrm{q}} < \tilde{\mathrm{q}}_{\mathrm{crit}}$) when the region of stable orbits is given by $\omega_\theta = 0$ ($\omega_r = 0$).

The resulted frequency profiles are given for four representative values of $\tilde{\mathrm{q}}$ lying in both attractive and repulsive regions. Namely we choose $\tilde{\mathrm{q}} = 1.0\,\mathrm{x}\,10^{11}$, $\tilde{\mathrm{q}} = 8.7\,\mathrm{x}\,10^{10}$,

$\tilde{\mathrm{q}} = -6.0\,\mathrm{x}\,10^{10}$ and $\tilde{\mathrm{q}} = -1.5\,\mathrm{x}\,10^{11}$. Absolute values of all used specific charge values are very low in comparison with $\tilde{\mathrm{q}} = 1.111\,\mathrm{x}\,10^{18}$ corresponding to matter consisting purely of ions of hydrogen.

4.1. Magnetic repulsion

The top left panel of Fig.4 displays behaviour of the investigated frequencies in the repulsive region for $\tilde{\mathrm{q}} = 1.0\,\mathrm{x}\,10^{11}$ ($\tilde{\mathrm{q}} > \tilde{\mathrm{q}}_{\mathrm{crit}}$), whereas Ω and ω_r are defined for all radii above the horizon. Ω exhibits a maximum and converges to 0 at the horizon, while ω_r monotonously grows diverging to infinity at the horizon. On the other hand ω_θ exhibits a maximum and falls to zero. Therefore, the region of stability of the circular orbits is defined by the radial coordinate r_{MISCO} where $\omega_\theta = 0$.

Different features are shown in the top right panel of Fig. 4 which illustrates the situation for $\tilde{\mathrm{q}} = 8.7\,\mathrm{x}\,10^{10}$ (still in the repulsive region but for $\tilde{\mathrm{q}} < \tilde{\mathrm{q}}_{crit}$). Contrary to the previous case there exists an interval of radial coordinate values over which Ω is not defined and where no circular orbits exist. Similarly, ω_r is discontinuous and the boundary of the stability region r_{MISCO} is now defined by the radial coordinate satisfying $\omega_r = 0$. Close to the horizon a new separate region appears where the circular orbits may again exist, although they are stable only with respect to radial perturbations. For the value of $\tilde{\mathrm{q}}$ used here, the upper boundary of such region slightly outreaches the minimal possible size of the stellar compact object, $R = 2.25M$.

Generally, for stable circular orbits in the repulsive region, ω_r increases with growing charge, while both Ω and ω_θ exhibit opposite behaviour. Both the orbital and vertical epicyclic frequencies are lower than the Keplerian frequency Ω_K, and the orbital frequency exceeds the epicyclic one. The influence of the Lorentz force enables extension of the region with stable circular orbits deep below the Schwarzschild $r_{\mathrm{GISCO}} = 6M$ and, surprisingly, even below the radius of the circular photon orbit $r_{ph} = 3M$.

4.2. Magnetic attraction

The bottom left panel of Fig.4 illustrates the behaviour of the orbital and epicyclic frequency profiles in the attractive region for $\tilde{\mathrm{q}} = -6.0\,\mathrm{x}\,10^{10}$. Ω displays a discontinuity that is characteristic for the whole attractive region and changes its sign at radius $r = 3M$ corresponding to the circular photon orbit. The region of inversely orbiting radially unstable circular non-geodesic orbits does not reach the horizon for the chosen value of $\tilde{\mathrm{q}}$. The boundary of the stability region r_{MISCO} is again defined by the radial coordinate where $\omega_r = 0$.

The frequency profiles constructed for $\tilde{\mathrm{q}} = -1.5\,\mathrm{x}\,10^{11}$, shown in the bottom right panel of Fig.4, are qualitatively somewhat different when compared with the previous magnetic attraction case. Even in the attractive region, sufficiently large values of negative $\tilde{\mathrm{q}}$ enable extension of the region of existence of the circular orbits down to the horizon, however, such orbits are, contrary to the case of magnetic repulsion, unstable with respect to both radial and vertical perturbations. The region of vertical stability

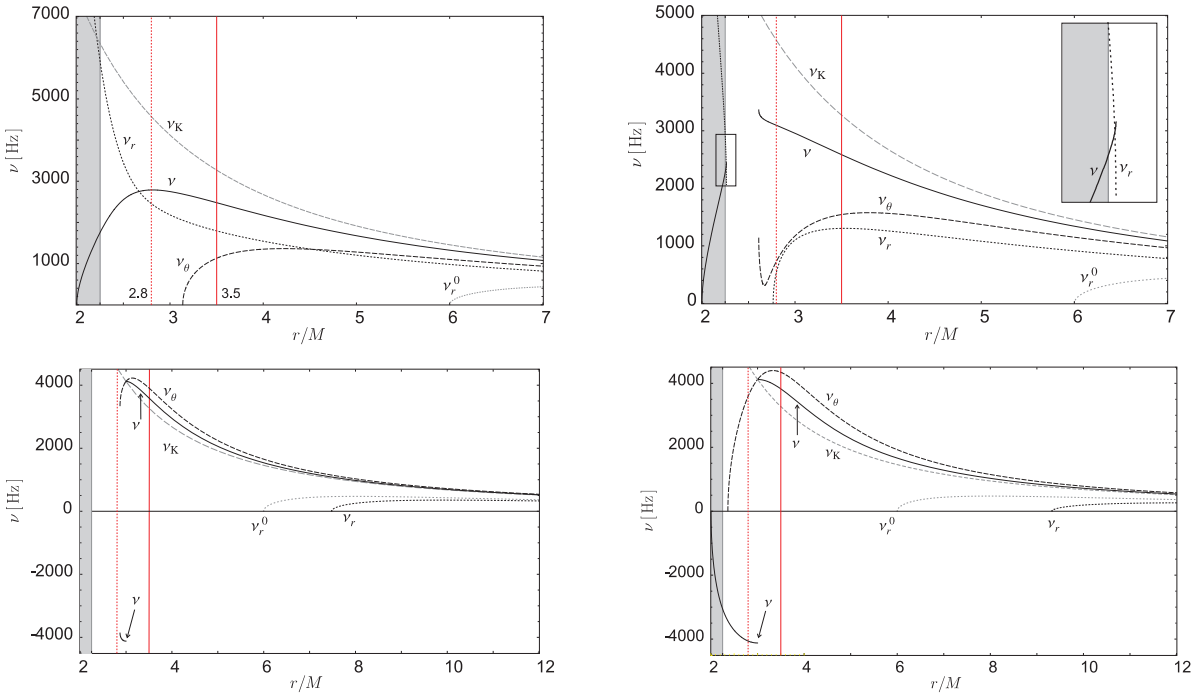

Figure 4. Illustration of the radial epicyclic, $\nu_r = \omega_r/(2\pi)$, vertical epicyclic, $\nu_\theta = \omega_\theta/(2\pi)$, and orbital, $\nu = \Omega/(2\pi)$, frequency behaviour in case of the intrinsic external dipole magnetic field $B = 10^7$ *Gauss* on the surface of the star with $M = 1.5\,M_\odot$ and $R = 4M$ compared to the pure Schwarzschild geodesic case (quantities $\nu_K = \nu_\theta^0$ and ν_r^0). The top panels illustrate the situation in the repulsive region, for $\tilde{\mathrm{q}} = 1.0\,\mathrm{x}\,10^{11}$ (left), and for $\tilde{\mathrm{q}} = 8.7\,\mathrm{x}\,10^{10}$ (right). Bottom panels show the behaviour of frequencies from the attractive region for $\tilde{\mathrm{q}} = -6.0\,\mathrm{x}\,10^{10}$ (left) and $\tilde{\mathrm{q}} = -1.5\,\mathrm{x}\,10^{11}$ (right).

is restricted from below by the radial coordinate for which $\omega_\theta = 0$, while the region of both radial and vertical stabilities is again limited by r_{MISCO} such that $\omega_r(r_{\mathrm{MISCO}}) = 0$.

Generally, in the attractive region the orbital and epicyclic frequency profiles exhibit opposite behaviour from that in the repulsive region. With increasing negative $\tilde{\mathrm{q}}$ the frequency ω_r decreases, while both Ω and ω_θ grow. Now both orbital and vertical epicyclic frequencies exceed the Keplerian one Ω_K, and, moreover, $\omega_\theta > \Omega$. However, at the circular photon orbit radius $r_{ph} = 3M$ both Ω and ω_θ coincide with the Keplerian angular velocity Ω_0 independently of $\tilde{\mathrm{q}}$. In the case of magnetic attraction the MISCO radius strongly draws apart from the Schwarzschild $r_{\mathrm{GISCO}} = 6M$ with growing $\tilde{\mathrm{q}}$.

Finally, we can conclude that at astrophysically relevant values of radial coordinate ($r > 3.5M$) sensitivity of ω_r to $\tilde{\mathrm{q}}$ is significantly higher than sensitivity of the two remaining frequencies for both attractive and repulsive magnetic interactions. This is qualitatively in accordance with what one would expect, as the Lorentz force acting on charged particles moving in the equatorial plane has only radial non-zero component.

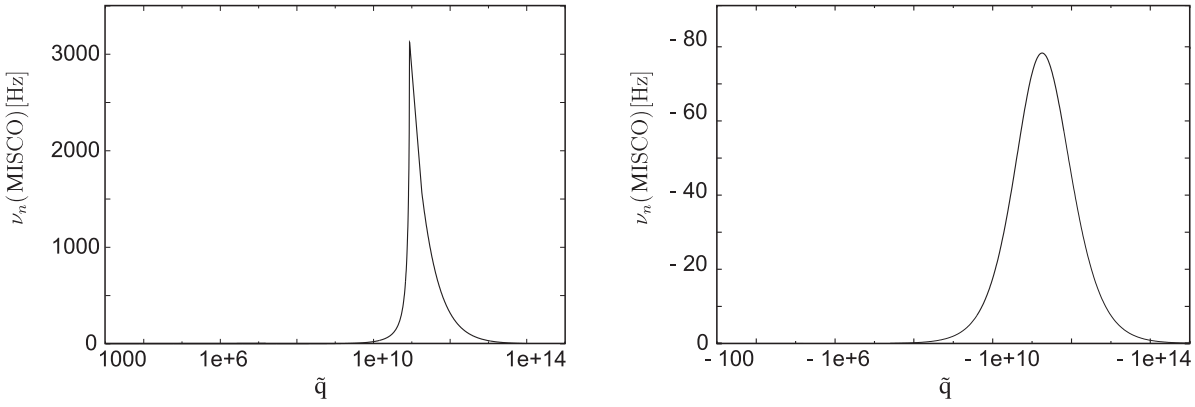

Figure 5. The behaviour of $\nu_{\rm n}$ at the innermost stable circular orbit in the presence of the intrinsic external dipole magnetic field with $B = 10^7$ *Gauss* on the surface of the test neutron star with $M = 1.5\,M_\odot$ and $R = 4M$ as a function of $\tilde{\rm q}$. Left: In the repulsive region the frequency has its maximum $\nu_{\rm n} = \nu^{max} = 3124$ Hz for $\tilde{\rm q} = \tilde{\rm q}_{crit}$ at the lowest stable circular orbit. Right: In the attractive region the frequency has its maximum $\nu_{\rm n} = 78.3$ Hz for $\tilde{\rm q} = -1.8\,{\rm x}\,10^{11}$ which corresponds to the shift of MISCO to 9.9 M.

5. Nodal precession

The presence of the Lorentz force violates the $\nu = \nu_\theta$ equality implied by the spherical symmetry of the background Schwarzschild geometry. In the repulsive region, both ν and ν_θ decrease as the specific charge $\tilde{\rm q}$ grows, while in the attractive region these frequencies increase with rising negative specific charge. However, ν_θ is changing faster than ν which gives rise to the nodal precession of the plane of the orbital motion. The nodal precession is present in addition to the relativistic precession of periastron having frequency $\nu_p(r) = \nu(r) - \nu_{\rm r}(r)$. The nodal precession frequency is given by the formula

$$\nu_{\rm n}(r) = \nu(r) - \nu_\theta(r). \tag{30}$$

This nodal precession of frequency $\nu_{\rm n}$ is qualitatively similar to the Lense-Thirring precession (LTP) occurring in rotating, axially symmetric spacetimes. For attractive magnetic interaction some of its features differ from those of the repulsive interaction. It is, however, common for both attractive and repulsive magnetic interactions that for a fixed value of $\tilde{\rm q}$ the frequency $\nu_{\rm n}(r)$ exhibits a maximum at the MISCO orbit and decreases with increasing r.

As follows from definition of $\nu_{\rm n}$ given by Eq.(30), for the attractive interaction the nodal precession induced by the Lorentz force has an opposite phase as compared to the LTP, reflected by its negative values on the right panel of Fig.3. It is interesting to plot $\nu_{\rm n}(r_{\rm MISCO})$ versus negative $\tilde{\rm q}$ for fixed μ and M (see the right panel of Fig.5). For the attractive magnetic interaction the nodal precession frequency $\nu_{\rm n}(r_{\rm MISCO})$ is small ($\nu_{\rm n} << 1$ Hz) except for a relatively narrow range of $\tilde{\rm q}$ (about $\tilde{\rm q} \sim -1.8\,{\rm x}\,10^{11}$) where it demonstrates a sharp maximum $\nu_{\rm n}(r_{\rm MISCO}) = 0.106\,\nu(r_{\rm MISCO})$.

For the repulsive magnetic interaction the nodal precession phase is consistent with the LTP phase. When $\tilde{\rm q} < \tilde{\rm q}_{\rm crit}$, the frequency $\nu_{\rm n}({\rm r}_{\rm MISCO})$ grows along with growing

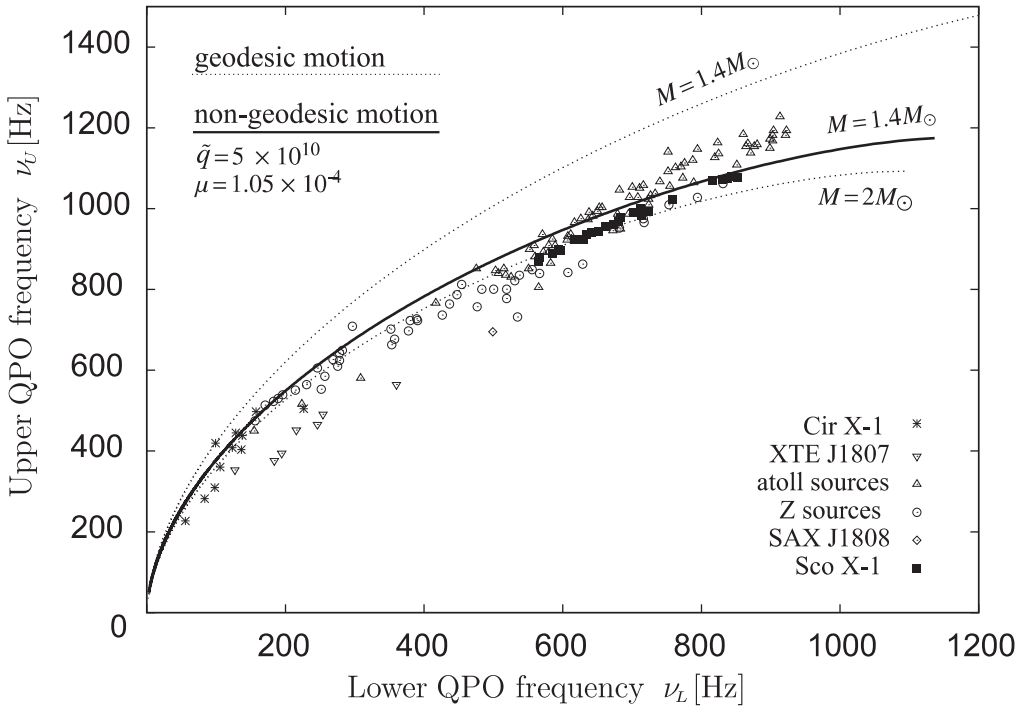

Figure 6. The RP model rough fits of the observational twin-peak kHz QPO data for a wide set of LMXBs. The thick solid curve refers to the case with $M = 1.4M_\odot$ and with the orbital and epicyclic frequencies being corrected by the presence of the Lorentz force induced by $\tilde{\mathrm{q}} = 5.0\,\mathrm{x}\,10^{10}$ and $\mu = 1.06\,\mathrm{x}\,10^{-4}\,m^2$. For illustration we also present fits corresponding to pure Schwarzschild geodesic case (thin dashed curves), namely for $M = 2M_\odot$ that was discussed by Belloni et al. (2007), and for $M = 1.4M_\odot$ for the comparison with the non-geodesic case.

$\tilde{\mathrm{q}}$. For MISCO orbits with $\tilde{\mathrm{q}} > \tilde{\mathrm{q}}_{\mathrm{crit}}$, there is $\nu_\theta(r_{\mathrm{MISCO}}) = 0$, the nodal precession frequency $\nu_{\mathrm{n}}(r_{\mathrm{MISCO}}) = \nu_K(r_{\mathrm{MISCO}})$ and decreases with growing $\tilde{\mathrm{q}}$. It is evident that for the repulsive interaction $\nu_{\mathrm{n}}(r_{\mathrm{MISCO}})$ exhibits a sharp maximum at $\tilde{\mathrm{q}} = \tilde{\mathrm{q}}_{\mathrm{crit}}$ which is identical with the ν^{max} of the lowest stable circular orbit (see the left panel of Fig.5).

6. Implications for the relativistic precession QPO model

The widely discussed relativistic precession QPO model identifies the frequencies of the lower and upper QPO peaks (ν_L and ν_U, respectively) as

$$\nu_L(r) = \nu(r) - \nu_{\mathrm{r}}(r), \quad \nu_U(r) = \nu(r). \tag{31}$$

It has been shown by Belloni et al. (2007) that these relations qualitatively well describe the trends presented in the observational data, but the characteristic mass of neutron stars in LMXBs obtained by such fits, $M \sim 2M_\odot$, is too high in comparison with the canonical value, $M \sim 1.4M_\odot$. Moreover, it was demonstrated by Török et al. (2007a) that decreasing the radial epicyclic frequency may in general notably improve the quality of fits based on the RP model. The significant reduction of $\nu_{\mathrm{r}}(r)$ along with keeping the

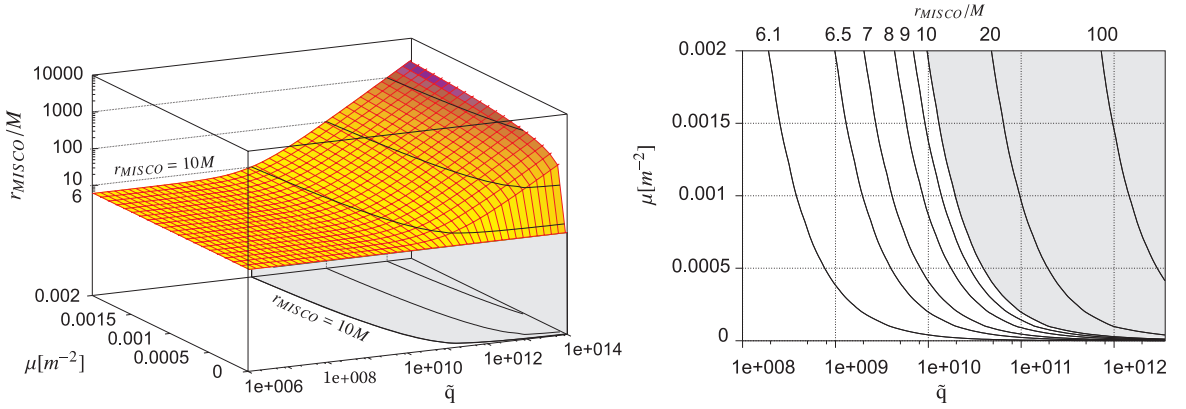

Figure 7. Left: The location of MISCO in the attractive region as a function of the test particle's specific charge $\tilde{q}$ and the intrinsic magnetic dipole moment μ of the star. The curves at the 3D-plot surface and their projections into the $\mu - \tilde{q}$ plane denote $r_{\rm MISCO} = 10M$, $100M$, $1000M$. Right: Projection of the astrophysically relevant region from the left panel to the $\mu - \tilde{q}$ plane with distinctive values of $r_{\rm MISCO}$.

other frequencies more or less the same well corresponds to above discussed features of the frequencies in the region of the attractive Lorentz force.

Consider an astrophysically relevant situation of a rather slowly rotating neutron star that possesses a dipole magnetic field and is orbited by a thin accretion disc consisting of charged test particles moving along nearly circular geodesics in the equatorial plane. In addition we assume the dipole magnetic field to be fully dominant in the total electromagnetic field in the vicinity of the star, so that the influence of magnetic field generated by the currents in the disc and the influence of the total disc charge are both negligible. This criterion is fulfilled if the specific charge of the material in the disc is very low. Further, such a configuration allows us to use the test particle approximation, and this is in agreement with the assumed rather small non-geodesic corrections to geodesic orbital motion.

Considering the RP model in the line with the corrected frequencies introduced above, the new fits can provide the characteristic neutron star mass close to $M \sim 1.4 M_\odot$. In Fig.6 we illustrate this finding for $\mu = 1.06\,\mathrm{x}\,10^{-4}\,m^2$ and $\tilde{q} = 5\,\mathrm{x}\,10^{10}$ when the innermost stable circular orbit is shifted to $r_{\rm MISCO} \sim 7M$. Such a rough fit for a wide set of LMXBs* is shown together with the fits for the pure Schwarzschild geodesic cases with $M = 2M_\odot$ (Belloni et al., 2007) and $M = 1.4M_\odot$. However, a detailed analysis for the particular LXMB sources should be carried out taking into account the above derived formulae♯.

Natural and simple implication of the RP model (and several other orbital models) identifies the highest observed frequency of the particular source with the orbital

* Data from Boutloukos et al. (2006); Wijnands et al. (2003); Linares et al. (2005); Belloni et al. (2007).
♯ Influence of the neutron star rotation (spin j) is shown to be relatively weak for both, radial and vertical, epicyclic frequencies, and it is quite negligible for small values of the spin ($j < 0.1$) (Török et al., 2008a).

frequency at the appropriate ISCO, and thus allows for the estimation of mass of the source (see, e.g, van der Klis, 2005; Lamb et al., 2007). A straightforward replacement of the GISCO orbital frequency by the corrected MISCO orbital frequency provides a significant decrease of the estimated mass.

Fig.7 illustrates high sensitivity of the MISCO orbit location on the intensity of the attractive magnetic interaction. With growing values of $\tilde{\mathrm{q}}$ or μ, r_{MISCO} rapidly draws apart from the radius of GISCO. In the case of the test neutron star with fixed $\mu = 1.06\,\mathrm{x}\,10^{-4}\,m^2$, we find that for $\tilde{\mathrm{q}} = 6.0\,\mathrm{x}\,10^{10}$ corresponding to bottom left panel of Fig. 4 there is $r_{\mathrm{MISCO}} = 7.48M$, while for $\tilde{\mathrm{q}} = 1.5\,\mathrm{x}\,10^{11}$ corresponding to bottom right panel of Fig. 4 we obtain $r_{\mathrm{MISCO}} = 9.32M$. For the extremal specific charge $\tilde{\mathrm{q}} = 1.111\,\mathrm{x}\,10^{18}$ corresponding to the case of matter purely consisting of ions of hydrogen, the location of MISCO orbit flies away to $r_{\mathrm{MISCO}} = 177864.76M$.

It is widely expected (e.g., Kluzniak et al., 1990; van der Klis, 2006) that magnetic field of the central compact objects in LMXBs should be given by the intrinsic exterior magnetic field, $B \in 10^6 \div 10^9$ Gauss. There are also several indices supporting the evidence of matter being accreted in the region with $r \leq 10M$ (see, e.g., van der Klis, 2006). Our results then imply that the specific charge related to the accreting matter should not exceed $\tilde{\mathrm{q}} \sim 1.86\,\mathrm{x}\,10^{12}$ $(1.87\,\mathrm{x}\,10^{11}, 1.90\,\mathrm{x}\,10^{10}, 1.91\,\mathrm{x}\,10^{9})$ for $B = 10^6\,Gauss$ $(10^7, 10^8, 10^9\,Gauss)$.

7. Conclusions

The aim of this paper is to study the influence of the Lorentz force generated by a magnetic field of a neutron star on the quasi-circular, epicyclic orbital motion. In particular we focus on the behaviour of non-geodesic orbital and epicyclic frequencies in dependence on the neutron star magnetic dipole moment and the specific charge of the orbiting matter.

In general, the Lorentz force may be of attractive or repulsive character depending on the sign of orbiting particle's specific charge, and the magnetic dipole moment and orbital velocity orientations. When the specific charge is large enough, the influence of both types of the force allows for the existence of circular orbits for all radii above the horizon. In the attractive region a discontinuity appears, only unstable circular orbits exists under the circular photon orbit at $r_{ph} = 3M$ being oppositely oriented to those located above r_{ph}. Surprisingly, in the repulsive region, the stable circular orbits associated with the radial and vertical epicyclic oscillations can extend below the circular photon orbit radius r_{ph}. A critical charge $\tilde{\mathrm{q}}_{crit}$ exists for given μ, corresponding to the lowest stable circular orbit at $r_{min}^{MISCO} = 2.73M$ with the highest possible orbital frequency Ω^{max} of stable circular motion ††. In contrast, inside the attractive region, the MISCO orbits always appear above $r_{\mathrm{GISCO}} = 6M$ and the r_{MISCO} can be substantially shifted above $r = 6M$. We can conclude that the presence of the Lorentz force strongly

††However, it should be stressed that for the repulsive magnetic interaction applicability of the stable orbits region has to be confronted with the location of the neutron star surface (see Appendix)

affects the location of the inner edge of the thin accretion disc.

In both repulsive and attractive regions of the magnetic interaction, the behaviour of the orbital and epicyclic frequency profiles is quite complicated, giving rise to two separated regions of the circular orbital motion for certain values of $\tilde{\mathrm{q}}$. Generally, for stable circular orbits in the repulsive region ω_r increases with growing specific charge, while both Ω and ω_θ decrease. In the attractive region, on the other hand, the frequencies exhibit opposite behaviour. For both regions of the magnetic interaction and astrophysically relevant values of radial coordinate ($r > 3.5M$) sensitivity of the radial epicyclic frequency ω_r to $\tilde{\mathrm{q}}$ is significantly higher than sensitivity of the two remaining frequencies.

The presence of the dipole magnetic field also violates the $\nu = \nu_\theta$ equality corresponding to the spherical symmetry of the background Schwarzschild geometry. As a result, nodal precession of the orbital motion plane arises, having opposite phase for attractive and repulsive magnetic interaction .

Orbital motion and related epicyclic frequencies have been considered by several authors as a key agent in their models of the high-frequency QPOs (Kato et al., 1998; Stella & Vietri, 1999; Kluźniak & Abramowicz, 2001; Török et al., 2005; Stuchlík & Kotrlová, 2009); in this paper we focused our attention to the relativistic precession QPO model. The models mostly assume geodesic motion although some non-geodesic corrections have been studied in the past, e.g., due to pressure gradient forces (Blaes et al., 2006, 2007; Šrámková et al., 2005; Straub & Šrámková, 2009), or due to diamagnetic forces in hot plasma interacting with the central compact object magnetic field (e.g., Vietri & Stella, 1998). However, non-geodesic corrections that arise from the interaction of dipole magnetic field with test particle's specific charge (i.e., the Lorentz force) have not been considered in this context yet. The formulae derived in this work therefore represent first attempt to describe the appropriate problem within the scope of general relativity. We have shown that such effects are of high importance and for attractive magnetic interaction they can improve significantly the fitting of high-frequency QPOs data for some LMXB sources by RP model.

Recently, sophisticated attempts appeared that are able to explain the high frequency QPOs by the models of oscillating toroidal disc (Rezzolla et al., 2003a,b; Lee et al., 2004; Li & Narayan, 2004; Montero et al., 2004; Zhang, 2004; Zanotti et al., 2005; Schnittman & Rezzolla, 2006) or by discoseismology of (warped) discs (Wagoner, 1999; Wagoner et al., 2001; Kato, 2004; Blaes et al., 2007). In all of these models, the orbital and epicyclic frequencies of the geodetical motion have an important role. It would be interesting to check, if the orbital and epicyclic frequencies of magnetic non-geodesic motion of slightly charged particles could be relevant for oscillations of slightly charged toroidal and warped discs.

In the present work we considered dipole magnetic field on the background of the spherically symmetric Schwarzschild geometry. Generalization of our results to axially symmetric spacetimes (e.g., Hartle-Thorne or Lense-Thirring solutions) that describe the influence of the neutron star rotation is the subject of our future study.

Acknowledgments

This work has been supported by the Czech grants LC 06014 (PB, ES) and MSM 4781305903 (ZS, GT). The authors (PB, ES, ZS) would like to thank to Copacabana Rio Hotel in Rio de Janeiro for great hospitality. The authors would like to thank dr. J. Kovář for useful discussions.

References

Abdujabbarov A A and Ahmedov B J 2009 *Astrophysics and Space Science* **321** 225
Abramowicz M A and Kluźniak W 2005 *Astrophysics and Space Science* **300** 127
Aliev A N and Galtsov D V 1981 *Gen. Rel. Grav.* **13** 899
Aliev A N 2008 *Proceedings of the Eleventh Marcel Grossmann Meeting on General Relativity (Berlin)* ed. H Kleinert, R T Jantzen and R Ruffini (Singapore: World Scientific) p 1057
Aschenbach B 2007 astro-ph/0710.3454
Bahcall S L, Bryan W, Selipsky S B 1989, *Nuclear Physics B*, **325/3** 606
Balek V, Bičák J and Stuchlík Z 1989 *Bull. Astronom. Inst. Czechoslovakia* **40** 133
Belloni T, Méndez M and Homan J 2007 *Mon. Not. R. Astron. Soc.* **376/3** 1133
Blaes O M, Arras P and Fragile P C 2006 *Mon. Not. R. Astron. Soc.* **369** 1235
Blaes O M, Šrámková E, Abramowicz M A, Kluźniak W and Torkelsson U 2007 *Astrophysical Journal* **665** 642
Blandford R D and Znajek RL 1977 *Mon. Not. R. Astron. Soc.* **179** 433
Braje T M & Romani R W 2001 *Astrophysical Journal* **550** 392
Boutloukos S, van der Klis M, Altamirano D, Klein-Wolt D, Wijnands R, Jonker P G and Fender R P 2006 *Astrophysical Journal* **653** 1435
Bičák J, Stuchlík Z and Balek V 1989 *Bull. Astronom. Inst. Czechoslovakia* **40** 65
Calvani M, de Felice F, Fabbri R and Turolla R 1982 *Nuovo Cimento B Serie* **67** 1
Chirenti C B M H, Rezzolla L 2007 *Class. Quantum Grav.* **24(16)** 4191
Glendenning N K 1997*Compact Stars: Nuclear Physics, Particle Physics, and General Relativity* (New York: Springer-verlag New York, Inc.)
Johnston M and Ruffini R 1974 *Phys. Rev. D* **10** 2324
Kato S, Fukue J and Mineshige S 1998 *Black Hole Accretion Disks* (Kyoto: Kyoto University Press)
Kato S 2004 *Publications of the Astronomical Society of Japan* **56** 905
van der Klis M 2005 *Astronomische Nachrichten* **326/9** 798
van der Klis M 2006 *Compact stellar X-ray sources* ed. W Lewin & M van der Klis. (Cambridge: Cambridge University Press) p 39
Kluźniak W, Michelson P and Wagoner R V 1990 *Astrophysical Journal* **358** 538
Kluźniak W and Abramowicz M A 2001 *Acta Physica Polonica* **B 32** 3605
Kovář J, Stuchlík Z and Karas V 2008 *Class. Quantum Grav.* **25** 095011
Lamb F K and Boutlokous S 2007 *Short-period Binary Stars: Observation, Analyses, and Results* ed. E F Milone, D A Leahy & D Hobill (Dordrecht: Springer)
Lee W H, Abramowicz M A, Kluźniak W 2004 *Astrophysical Journal Letters* **603** L93
Li L X and Narayan R 2004 *Astrophysical Journal* **601** 414
Linares M, van der Klis M, Altamirano D and Markwardt C B 2005 *Astrophysical Journal* **634** 1250
Mazur P O, Mottola E 2004 *Proc.Nat.Acad.Sci* **101** 9545
Miller J C, Shahbaz T, Nolan L A 1998 *Mon. Not. R. Astron. Soc.* **294** L25
Miller J M 2007 astro-ph/0705.0540
Mobarry C M and Lovelace R V E 1986 *Astrophysical Journal* **309** 455
Montero P J, Rezzolla L, Yoshida S 2004 *Mon. Not. R. Astron. Soc.* **354** 1040
Petterson J A 1974 *Phys. Rev. D* **10** 3166

Pétri J 2005 *Astronomy and Astrophysics* **443/3** 777
Prasanna A R 1980 *Nuovo Cimento* **3/3** 1
Prasanna A R and Sengupta S 1994 *Physics Letters A* **193** 25
Prasanna A R and Vishveshwara C V 1978 *Pramana* **11** 359
Preti G 2004 *Class. Quantum Grav.* **21** 3433
Rezzolla L, Ahmedov B J and Miller J C 2001 *Mon. Not. R. Astron. Soc.* **322** 723
Rezzolla L, Ahmedov B J and Miller J C 2001 *Found.Phys.* **31** 1051
Rezzolla L, Yoshida S and Maccarone T J 2003 *Mon. Not. R. Astron. Soc.* **344** L37
Rezzolla L, Yoshida S and Zanotti O 2003 *Mon. Not. R. Astron. Soc.* **344** 978
Schnittman J D and Rezzolla L 2006 *Astrophysical Journal Letters* **637** L113
Stella L and Vietri M 1998 *Astrophysical Journal Letters* **492** L59
Stella L and Vietri M 1999 *Phys. Rev. Letters* **82** 17
Stella L and Vietri M 2002 *Proceedings of the MGIXMM Meeting held at The University of Rome "La Sapienza", 2-8 July 2000* Part A ed. V G Gurzadyan, R T Jantzen and R. Ruffini (World Scientific Publishing) p 426
Šrámková E, Torkelsson U and Abramowicz M A 2005 *Astronomy and Astrophysics* **467/2** 641
Straub O and Šrámková E 2009 *Class. Quantum Grav.* **2** 055011
Stuchlík Z and Hledík S 1998 *Acta Physica Slovaca* **48** 549
Stuchlík Z, Bičák J and Balek V 1999 *Gen. Relativity and Gravitation* **31** 53
Stuchlík Z 2000 *Acta Physica Slovaca* **50** 219
Stuchlík Z, Hledík S, Šoltés J and Ostgaard E 2001 *Phys. Rev. D* **64(4)** 044004
Stuchlík Z, Konar S, Miller J and Hledík S 2008 *Astronomy and Astrophysics* **489(3)** 963
Stuchlík Z and Kotrlová A 2009 *Gen. Rel. Grav.* **41(6)** 1305
Stuchlík Z, Török G, Hledík S and Urbanec M 2009 *Class. Quantum Grav.* **26(3)** 035003
Stuchlík Z, Kovář J and Karas V 2009 *Cosmic Magnetic Fields: From Planets, to Stars and Galaxies, Proceedings of the International Astronomical Union, IAU Symposium* **259** 125
Török G, Abramowicz M A, Kluźniak W and Stuchlík Z 2005 *Astronomy and Astrophysics* **436** 1
Török G and Stuchlík Z 2005 *Astronomy and Astrophysics* **437** 775
Török G, Bakala P, Stuchlík Z and Šrámková E 2007 *Proceedings of RAGtime 8/9:Workshop on black holes and neutron stars (Opava)* **8/9** ed. Z Stuchlík & S Hledík (Opava: Silesian University in Opava) p 489
Török G, Stuchlík Z and Bakala P 2007 *Central European Journal of Physics* **5/4** 457
Török G, Bakala P, Stuchlík Z and Čech P 2008 *Acta Astronomica* **58** 1
Török G, Abramowicz M A, Bakala P, Bursa M, Horák J, Kluźniak W, Rebusco P and Stuchlík Z 2008 *Acta Astronomica* **58** 15
Török G, Abramowicz M A, Bakala P, Bursa M, Horák J, Rebusco P and Stuchlík Z 2008 *Acta Astronomica* **58** 113
Vietri M and Stella L 1998 *Astrophysical Journal* **503** 350
Vokrouhlický D and Karas V 1990 *Astronomy and Astrophysics* **243** 165
Wagoner R V 1999 *Phys. Rep.* **311** 259
Wagoner R V, Silbergleit A S and Ortega-Rodríguez M 2001 *Astrophysical Journal Letters* **559** L25
Weber F 1999 *Pulsars as Astrophysical Laboratories for Nuclear and Particle Physics* (Philadelphia: Institute of Physics Publishing Bristol and Philadelphia)
Wasserman I and Shapiro S L 1983 *Astrophysical Journal* **265** 1036
Wijnands R, van der Klis M, Homan J, Chakrabarty D, Markwardt C B and Morgan E H 2003 *Nature* **424** 44
Zanotti O, Font J A, Rezzolla L and Montero P J 2005 *Mon. Not. R. Astron. Soc.* **356** 1371
Zhang C 2004 *Astronomy and Astrophysics* **423** 401
Znajek R 1976 *Nature* **262** 270

Appendix A. Radius and magnetic dipole moment of neutron stars

Presented analysis of circular and epicyclic motion is relevant in the exterior of the neutron star only. Therefore, it is very important to fix the neutron star radius R. In order to obtain a complete view of the motion, we study its properties down to $R = 2.25M$ that represents an innermost limit on the neutron star radius, being given by the limit on existence of internal (but unrealistic) Schwarzschild spacetime with uniformly distributed energy density - for such configuration the central pressure diverges (Stuchlík, 2000; Stuchlík et al., 2001). † On the other hand, realistic equations of state for both neutron and quark stars put the neutron (quark) star radius into the interval $(3-5)M$; we take intermediate value of $R = 4M$ for our test neutron star. Most of the realistic equations of state put the lower limit on the neutron star radius at the value of $R = 3.5M$ (Glendenning, 1997) which is considered here as a limit radius of astrophysically plausible neutron stars. Nevertheless, existence of extremely compact neutron stars with $R < 3M$ is still discussed and is not excluded; for example, realistic models of the so called Q-stars allow $R \sim 2.8M$ (Bahcall et al., 1989; Miller et al., 1998; Stuchlík et al., 2009a). Clearly, in vicinity of extremely compact neutron stars the exotic phenomena related to the magnetic repulsion under the photon circular orbit could be observed, giving thus signature of existence of these extreme objects.

Intrinsic magnetic dipole moment of a neutron star can be obtained from the presumed magnetic field strength at the neutron star surface. The orthonormal basis of local static observers in the Schwarzschild spacetime reads

$$e_{\hat{t}} = \left\{\frac{1}{\eta(r)}, 0, 0, 0\right\}, \qquad e_{\hat{r}} = \left\{0, \eta(r), 0, 0\right\}, \tag{A.1}$$

$$e_{\hat{\theta}} = \left\{0, 0, \frac{1}{r}, 0\right\}, \qquad e_{\hat{\phi}} = \left\{0, 0, 0, \frac{1}{r\,\sin\theta}\right\}.$$

Locally measured magnetic field strength is given by the projection of the Maxwell tensor into the orthonormal basis of a static observer $F_{\hat{\alpha}\hat{\beta}} = e^{\mu}_{\hat{\alpha}} e^{\nu}_{\hat{\beta}} F_{\mu\nu}$, at the surface of the star. For such an observer located at the equator of the star with radius R, the magnetic field three-vector has only one nonzero component,

$$B^{\hat{\theta}} = F_{\hat{r}\hat{\phi}} = \frac{\eta(R)}{R}\, F_{r\phi}\,. \tag{A.2}$$

Therefore, using Eqs. (5) and (7), one may write

$$\mu = \frac{4M^3 R^{3/2}\sqrt{R-2M}}{6M(R-M) + 3R(R-2M)\log\eta\,(R)^2}\, B^{\hat{\theta}}\,. \tag{A.3}$$

For a neutron star with a rather weak magnetic field strength, $B = 10^7\ Gauss \simeq 2.875\,\mathrm{x}\,10^{-16}\,m^{-1}$, mass $M = 1.5M_\odot$ and radius $R = 4M$, we have $\mu = 1.06\,\mathrm{x}\,10^{-4}\,m^2$ ($B\,[cm^{-1}] = (G^{1/2}/c^2)\,B\,[Gauss] \simeq 2,875\,\mathrm{x}\,10^{-25}\,B\,[Gauss]$). We have used neutron

† Admitting existence of hypothetical gravastars (Mazur & Mottola, 2004; Chirenti & Rezzolla, 2007) we can extend our analysis down to the gravitational radius $R_g = 2M$.

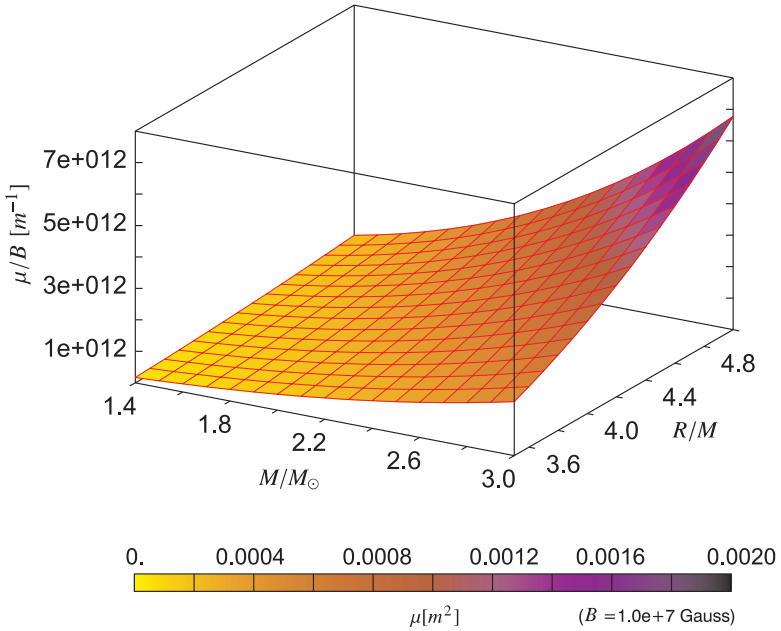

Figure A1. Intrinsic magnetic dipole moment μ of the star as a function of the star radius R and mass M for a fixed magnetic field strength B at the star surface. The z-axis is scaled in relative units of μ/B while the colour scaling at the 3D-plot surface shows values of μ for $B = 10^7\ Gauss = 2.875\,\mathrm{x}\,10^{-16}\,m^{-1}$.

stars of such parameters as the test model for our analysis. Dependence of the magnetic dipole moment μ (expressed in terms of the surface value of the magnetic field strength B) on the neutron star mass M and its radius R is illustrated in Fig A1.

The electromagnetic four-potential (4) used here corresponds to the case of magnetic dipole moment connected to the central compact object (neutron star). In the case of Schwarzschild black holes with magnetic field generated by a current loop in the accretion disc (Petterson, 1974), the discussed solution is valid only for particles orbiting at the radius higher than the loop radius. Discussion on the so-called internal solution of the four-potential and orbits of the particles below the loop radius can be found in Preti (2004).